

UHE GAMMA RAY OBSERVATIONS WITH THE KGF AIR SHOWER ARRAY §

B.S.ACHARYA, P.N.BHAT, S.G.KHAIRATKAR, M.R.RAJEEV, M.V.S.RAO, S.SINHA*, K.SIVAPRASAD, B.V.SREEKANTAN, S.C.TONWAR, P.R.VISHWANATH AND K.VISWANATHAN

Tata Institute of Fundamental Research, Homi Bhabha Road, Colaba, Bombay 400 005, India

Results on search for point sources based on the data collected from October 1984 to January 1987 from the EAS array at KGF are presented. The array has a pointing accuracy of better than 1.5° to look at point sources. We present upper limit on the long term flux of gamma rays from Cygnus-X3 and report possible episodic emission from Cyg X-3 and Her X-1 during 1985.

1. INTRODUCTION

Since the discovery of Cyg X-3 as a ultra high energy (UHE) gamma ray source by the Kiel group¹ and subsequent confirmation by the Haverah Park group², search for such sources has gained importance as these are the likely sources of cosmic rays also. We have been operating an extensive air shower array specially designed to look for such sources since the end of 1984. We present here the salient features of the array and the results obtained so far.

2. EXPERIMENTAL SET UP

For a proper study of point sources of UHE gamma rays an EAS array should have the following features:

- (i) determination of the arrival angle of showers with a high accuracy,
- (ii) large collection area and
- (iii) large area muon detectors to establish the nature of the radiation.

An array with all these features has been operating at Kolar Gold Fields, India. The array^{3,4} consists of 127 plastic scintillation detectors, each of 1 m^2 area and 7 muon detectors of threshold energy 1 GeV, each having an area of 28.8 m^2 . The scintillators are arranged in a hexagonal pattern with a spacing of 20 m between

neighbouring detectors. The detectors extend up to 120 m from the center, covering an area of $4.3 \cdot 10^4 \text{ m}^2$. The innermost 61 detectors are instrumented for both timing and density measurements while the rest measure only density. The threshold particle density for triggering the timing detector is kept at 0.3 to minimize rise time effects. The air shower trigger is provided by a coincidence of any three (among the innermost 61) neighbouring detectors forming an equilateral triangle of side 20 m, in which the particle density exceeded 1.5. The trigger rate is 1 Hz. A stable 5 MHz Oscillo-quartz crystal provided real time information with an uncertainty of about 1 ms. Six of the muon detectors are located at the vertices of a hexagon of side 60 m and the seventh at its center, which coincides with the center of the array. Each muon detector consists of two layers of 48 proportional counters each, located under 600 g cm^{-2} of concrete and separated by 4 radiation lengths of brick. An on-line LSI-11 microprocessor recorded the events and also continuously monitored the performance of all the detectors.

The data used in the present work was collected from October 1984 to January 1987, during which only the innermost 61 detectors were operating with an enclosed area of $1.6 \cdot 10^4 \text{ m}^2$ and the muon detectors were not yet fully commissioned.

§ Paper presented at the Workshop on Physics and Experimental Techniques of High Energy Neutrinos and VHE and UHE Gamma-Ray Particle Astrophysics , Little Rock, U.S.A., 11-13 May, 1989.

* Present address: Technical Physics Division, ISRO Satellite Center, Airport Road, Vimanapura P.O., Bangalore 560 017.

3. METHOD OF ANALYSIS

Shower size, N_e , and age parameter, s , were determined for each event in the usual way by fitting the Nishimura-Kamata-Greisen (NKG) function for the lateral distribution of electrons to the observed densities of particles. The arrival direction was obtained by fitting a plane shower front to the observed time delays taking into account the variation of disc thickness with core distance. The angular accuracy of the array was obtained by comparing the estimated zenith angles of the same set of showers using two separate groups of timing detectors (the odd numbered and the even numbered detectors) which spatially overlap. The angular accuracy thus obtained is 0.5° in zenith angle for showers of size $> 5 \cdot 10^4$ particles. Details of the analysis were given elsewhere^{3,4}. However, analysis of showers generated artificially with observed curvature but analysed with a plane front, has shown that 50% of showers are contained in a cone of half angle 1.5° around the true direction and 90% within 3° .

3.1. Estimation of background

Air showers have a fairly steep zenith angle distribution and therefore when one is looking for excess events from the source compared to background, care should be taken to make sure that the source and the background events are collected during the same time (to take care of run gaps) in the same zenith angle interval³. We have done this in the following way. At any instant we know the position of the source in the sky viz its zenith angle θ_s and azimuth ϕ_s . For an angular acceptance θ_a , we can draw an annulus in the sky formed by the rings with $\theta = \theta_s - \theta_a$ and $\theta = \theta_s + \theta_a$. At any instant we accept only events from this annulus and call them 'source' events if the space angle they make with the source is less than θ_a and 'background' otherwise. Since the background events come from a larger solid angle they are weighted in the ratio of 'source' solid angle to the 'background' solid angle. This ensures that the zenith angle and phase coverage is the same for both source and background, and gaps in run time or short run times do not matter. As the solid angle for the background events is about 40 times

larger than that for the source events, the background was determined with high statistical accuracy.

For further analysis, showers whose cores were within 70 m from the centre of the array and zenith angles less than 50° were accepted. Since the sources cover a wide zenith angle region, showers of a given observed threshold size but arriving at different zenith angles correspond to different primary energies since they develop through different atmospheric depths. While this does not affect the background estimates since it is calculated using showers recorded in the same zenith angle region during the same time as the source events, the threshold primary energy becomes ill defined. In order to avoid this, a vertical equivalent size (VES) is calculated for each shower using an absorption mean free path of 185 g cm^{-2} . Showers with $\text{VES} > 1.5 \cdot 10^5$, for which the array is fully efficient, were accepted for further analysis. The corresponding primary energy is $1.6 \cdot 10^{15} \text{ eV}$.

4. RESULTS

4.1. Cygnus X-3

Data collected over the entire period under consideration do not show any excess from the direction of the source, with $\theta_s = 3^\circ$. The number of events from the direction of the source is 1598 against an expected background of 1704.4, leading to a 2.6σ deficiency. The 3σ upper limit, based on this observation during the period October 1984 to January 1987, for the time averaged flux of gamma rays of energy $> 1.6 \cdot 10^{15} \text{ eV}$ is $1.8 \cdot 10^{-14} \text{ cm}^{-2} \text{ s}^{-1}$. The phasogram obtained using the van der Kliss ephemeris is shown in Fig. 1. There is no significant excess in any of the phase bins.

However, during April - May 1985, the number of events from the source direction is 207 while the background is 191.7, amounting to a 1.1σ excess. The phasogram for this period is shown in Fig. 2. In the phase bin 0.5 - 0.6, the number of source events is 38 and the background is 21.2, leading to a 3.7σ excess. All the 16 events in the DC excess appear in the phase excess. Considering that there are 17 such two month periods in the data and 10 phase bins, the overall

chance probability is 0.02.

4.2. Her X-1

Data collected over the entire period under consideration do not show any significant steady excess (121

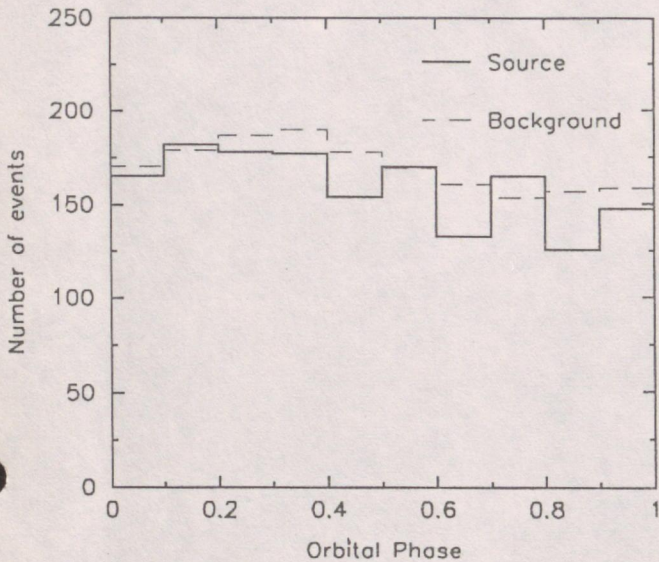


Fig. 1. Orbital Phsogram of air showers arriving from the direction of Cygnus X-3 during the period October 1984 to January 1987. No significant excess is seen in any of the phase bins.

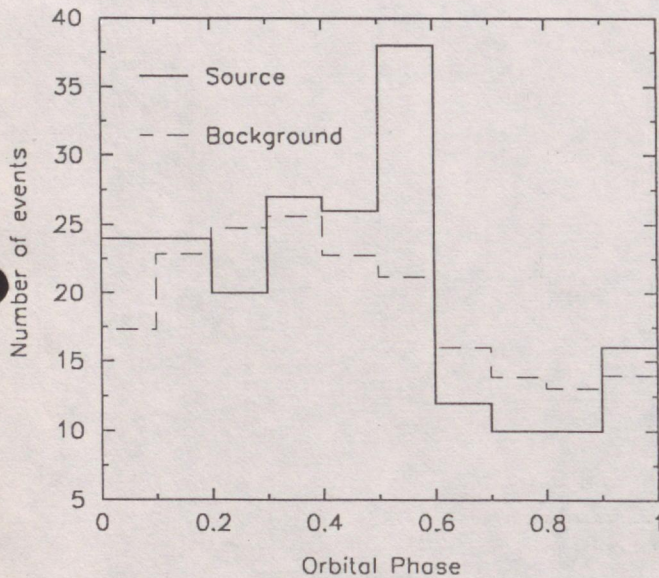


Fig. 2. Orbital phsogram of air showers arriving from the direction of Cygnus X-3 during the period April - May, 1985. A 3.7σ excess is seen in the phase bin 0.5 - 0.6. The overall chance probability, taking all degrees of freedom into account, is 0.02.

source events against an expected background of 113.8) or excess in any orbital phase region. To look for short episodes of activity, the data were divided into 6 roughly equal groups, essentially decided by the number of tapes on which they were written. In one of these groups comprising of 17 runs covering the period May 23, 1985 to July 20, 1985, the number of events within 1.5° from the source direction is 20 against a background of 10.5 events amounting to a 3σ excess over the background. The orbital phsogram for these events obtained using the ephemeris given by Voges et al⁵ ($p = 1.70016799$ d with phase, $\Phi = 0$ at epoch JD 2 443 357.8711) is shown in Fig 3. There are 7 events in the phase bin 0.7-0.8 against an expected background of 1.3 events. The Poisson probability that this occurrence is due to chance is $4.4 \cdot 10^{-4}$. Considering that there are 10 phase bins and 6 data sets, the probability of one or more phase bins showing such an excess in the entire data is $60 \times 4.4 \cdot 10^{-4} = 0.026$. It may be noted that out of the nine events in the steady excess, six are in this phase bin.

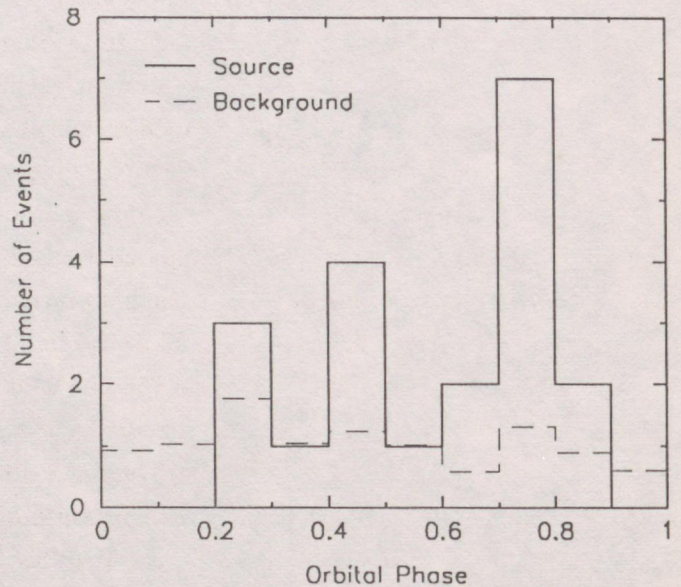


Fig. 3. Orbital phsogram of air showers arriving from the direction of Hercules X-1 during the period May 23 to July 20, 1985. There are 7 events in the phase bin 0.7 - 0.8 against an expected background of 1.3. The overall chance probability, taking all degrees of freedom into account, is 0.026.

It is interesting to note that the orbital phase interval 0.7-0.8 occurred only on two days, on May 24 and June 22, 1985 at 35-day phases of 0.095 and 0.923, just around the onset of 'High On' state, and on both these days excess events from the source are seen. The respective source and background events on these two days are 4, 0.23 and 3, 1.09. Thus it appears that Hercules X-1 is active in emitting UHE gamma rays in this orbital phase during May 23, 1985 to July 20, 1985.

With 6 events recorded in the phase interval 0.7-0.8 during an on-source time of 55.34 hours over an area of $1.54 \cdot 10^8 \text{ cm}^2$ and with 50% of the source events contained within the accepted angular region of 1.5° around the source direction, the time averaged flux of gamma rays of energy $> 1.6 \cdot 10^{15} \text{ eV}$ is estimated to be $(3.9 \pm 1.6) \cdot 10^{-13} \text{ photons cm}^{-2} \text{ s}^{-1}$. The corresponding source luminosity is $2.9 \cdot 10^{36} \text{ ergs s}^{-1}$, assuming isotropic emission and a source energy spectrum of $E^{-2} \text{ dE}$ with a high energy cut off of 10^{16} eV . The exposure time for the phase interval 0.7-0.8 was 4.12 hours and the flux and luminosity during this phase interval are $5.2 \cdot 10^{-12} \text{ cm}^{-2} \text{ s}^{-1}$ and $3.9 \cdot 10^{37} \text{ ergs s}^{-1}$ respectively.

It is interesting to note that the most significant episode of pulsed emission of gamma rays of energy $> 0.6 \text{ TeV}$ seen by the Whipple Observatory group^{6,7} is on June 16, 1985, which is within our period of observation.

5. CONCLUSIONS

During the period October 1984 to January 1987, we have not seen any excess in DC or in any phase from the direction of Cyg X-3. The 3σ upper limit for the flux of gamma rays of energy $> 1.6 \cdot 10^{15} \text{ eV}$ is $1.8 \cdot 10^{-14} \text{ cm}^{-2} \text{ s}^{-1}$. There seems to be episodic emission in the phase 0.5 - 0.6 during April - May, 1985, with a significance of 0.02. There appears to be episodic emission from Her X-1 also during May 23 to July 20, 1985 in the orbital phase 0.7 - 0.8 just at the onset of the 'High On' state.

ACKNOWLEDGMENTS

We thank B.K.Chatterjee, A.V.John, R.Mahalingam, B.K.Nagesh, N.S.Prasad, Ramesh Babu Raj, Shobha Rao, V.Ramu, C.V.Raisinghani, A. Reddy, P.Reddy, A.J.Stanislaus, S.Swaminathan, Suresh Upadhyaya, P.Unnikrishnan, M.Venkateshwarlu, B.L.Venkateshamurthy and R.P.Verma for their assistance in building and operation of the array and analysis of data. It is a pleasure to acknowledge the kind cooperation of the Chairman and Managing Director of Bharat Gold Mines Limited and his staff.

REFERENCES

1. M.Samorski and W.Stamm, *Ap. J. Lett.*, 268 (1983) L17.
2. J.Lloyd-Evans et al., *Nature*, 305 (1983) 784.
3. P.N.Bhat et al., in *Techniques in Ultra High Energy Gamma Ray Astronomy*, eds. R.J.Protheroe and S.A.Stephens (University of Adelaide, 1985) pp. 1-7.
4. P.N.Bhat et al., in *Very High Energy Gamma Ray Astronomy*, ed. K.E.Turver (Reidel, 1987) pp. 271-274.
5. W.Voges, P.Kahabka, H.Ögelman, W.Pietsch and J.Trümper, *Space Science Rev.*, 40 (1985) 339.
6. P.W.Gorham et al., *Ap. J. Lett.* 308 (1986) L11.
7. P.W.Gorham et al., in *Very High Energy Gamma Ray Astronomy*, ed. K.E.Turver (Reidel, 1987) pp. 125-130.

UHE GAMMA RAY OBSERVATIONS WITH THE KGF AIR SHOWER ARRAY

B.S.ACHARYA, P.N.BHAT, S.G.KHAIRATKAR, M.R.RAJEEV, M.V.S.RAO,
S.SINHA, K.SIVAPRASAD, B.V.SREEKANTAN, S.C.TONWAR,
P.R.VISHWANATH AND K.VISWANATHAN

*Tata Institute of Fundamental Research
Homi Bhabha Road
Bombay 400 005
India*

ABSTRACT. Preliminary results based on the data collected from October 1984 to January 1987 from the 61 detector EAS array at KGF are presented. The array has a pointing accuracy of better than 1.5° to look at point sources. From April 1986-87 muon detectors of total area 200 m^2 have also been in operation. We present upper limits on the flux of gamma rays from CYGNUS-X3 and demonstrate the usefulness of our muon detectors in improving the signal to noise ratio for gamma ray showers, if conventional interaction models are valid.

1. Experimental Set Up

For a proper study of point sources of ultra high energy (UHE) gamma rays an extensive air shower (EAS) array should have the following features:

- (i) determination of the arrival angle of showers with a high accuracy,
- (ii) large collection area

and

- (iii) large area muon detectors to establish the nature of the radiation.

An array with all these features has been operating at Kolar Gold Fields (KGF), India. The array consists of 127 plastic scintillation detectors, each of 1 m^2 area and 7 muon detectors of threshold energy 1 GeV, each having an area of 30 m^2 (Bhat *et al*, 1985, 1986). The scintillators are arranged in a hexagonal pattern with a spacing of 20 m between neighbouring detectors. The detectors extend up to 120 m from the center, covering an area of $4.3 \cdot 10^4 \text{ m}^2$. The innermost 61 detectors are instrumented for both timing and density measurements while the rest measure only density. The threshold particle density for triggering the timing detector is kept at 0.3 to minimize rise time effects. The air shower trigger is provided by a coincidence of any three (among the innermost 61) neighbouring detectors forming an equilateral triangle of side 20 m, in which the particle density exceeded 1.5. The trigger rate is 1 Hz. A stable 5 MHz Oscilloquartz crystal provided real time information with an uncertainty of about 1 ms. Six of the muon detectors are located at the vertices of a hexagon of side 60 m and the seventh at its center, which coincides with the center of the array. Each muon detector consists of two layers of 48 proportional counters each, located under 600 g cm^{-2} of concrete and separated by 4 radiation lengths of brick. An on-line LSI-11 microprocessor recorded the events and also continuously monitored the perform-

Paper presented at the INTERNATIONAL SCHOOL OF COSMIC-RAY ASTROPHYSICS,
6th Course: Cosmic Gamma Rays and Cosmic Neutrinos, 20-30 April 1988, Erice, Italy.

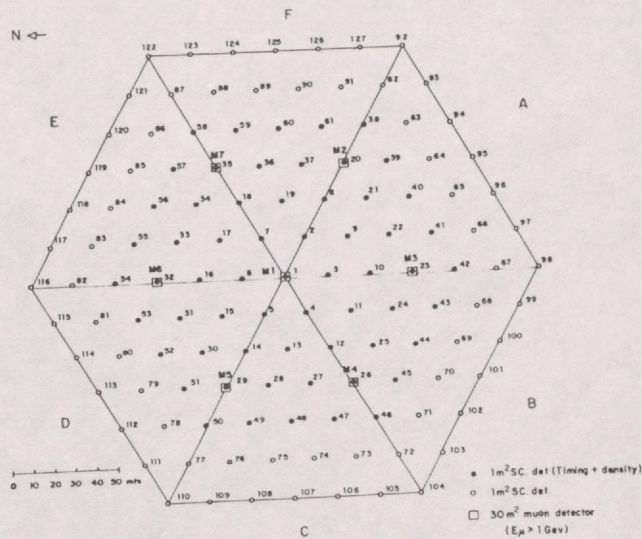


Figure 1. The Extensive Air Shower Array at Kolar Gold Fields.

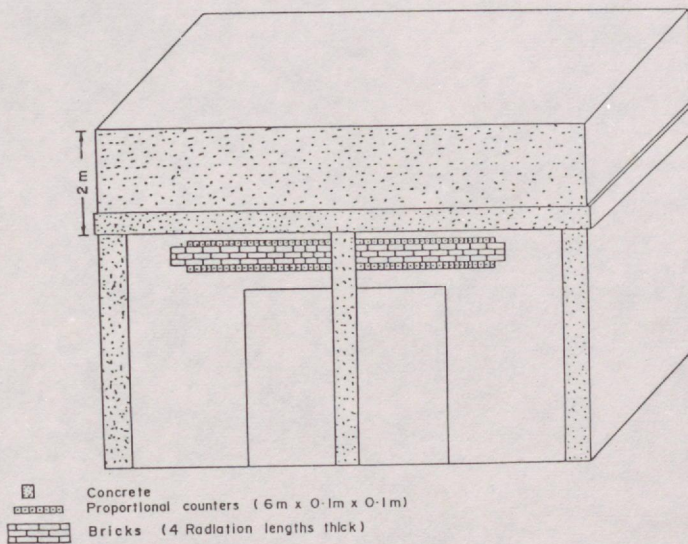


Figure 2. A schematic view of a muon detector in the KGF array.

ance of all the detectors. Fig. 1 shows the EAS array and Fig. 2 the schematic diagram of the muon detector.

2. Data Analysis

2.1. DETERMINATION OF ANGLE OF ARRIVAL

Conventional EAS studies fit a plane front to the shower and estimate the angle of arrival from the observed set of times of arrival. If (x_i, y_i, z_i) were the coordinates of the i th detector, l, m, n the direction cosines of the axis of the shower and t_i , the time at which the detector responded (at the $0.3 / \text{m}^2$ density level, say) then

$$lx_i + my_i + nz_i + c(t_i - t_0) = 0 \quad (1)$$

is the equation relating them. Here t_0 is the reference time and is the time at which a fictitious detector at the origin of the coordinate system would have responded. Also, note that l, m and n are related by $l^2 + m^2 + n^2 = 1$. Usually, the sum ψ^2 , defined by

$$\psi^2 = \sum \omega_i \{lx_i + my_i + nz_i + c(t_i - t_0)\}^2 \quad (2)$$

the summation running over all the available detectors, is minimised to determine the free parameters l, m and t_0 . ω_i is the weight given to the i th timing measurement, t_i , and includes the expected fluctuations in the measurement due to the finite shower disc thickness and instrumental uncertainties. However, there are observations (Eames *et al* 1987) as well as simulations that have shown that the shower disc shows deviations from a plane and that there is a linear deviation of the times of arrival of the particles with respect to the plane perpendicular to the shower axis, the deviation increasing with the distance from the core. The shower front, thus, approximates to a cone moving down along the axis. In this case equation (2) can be modified to

$$\psi^2 = \sum \omega_i \{ lX_i + mY_i + nZ_i + c(t_i - T_0 - br_i / N_i^{0.5}) \}^2 \quad (3)$$

and minimization is done with l, m, T_0 and b as free parameters. X_i, Y_i and Z_i are the coordinates of the detector with respect to the core $(x_0, y_0, 0.0)$ and T_0 is the time of arrival of the shower cone at a fictitious detector at the core. The N_i term implies that the mean deviation from the plane decreases with the number of particles in the detector. Our data also supports the observations of Eames *et al*, with a difference in the behaviour at small distances from the core, as has been established by using the following procedure. For each shower, the detector having the largest density and the hexagon of detectors surrounding it are used to fit a plane front to estimate the arrival angle. Only those showers with the highest recorded density within 60 m from the center of the array were used for this purpose. From the plane fit one estimated the expected time of arrival of particles in the detectors not used for the fit and constructed distributions of the observed minus expected times of arrival as a function of distance from the core. The core was obtained from a NKG fit to the observed densities and using the angle of arrival based on the plane fit. As seen from Fig. 3, the mean of the distribution is linearly increasing with distance and the dispersion is also an increasing function of the distance. The latter fact, supporting Linsley's formulation of the variation of the thickness of the shower disc with core distance, is used in writing expressions for the ω_i used in minimizing equation (3). Note that in Fig. 3, we see that at zero distance the mean deviation extrapolates to a small negative value. This is the displacement of the fitted average plane towards the rear of the shower front near the core, with a

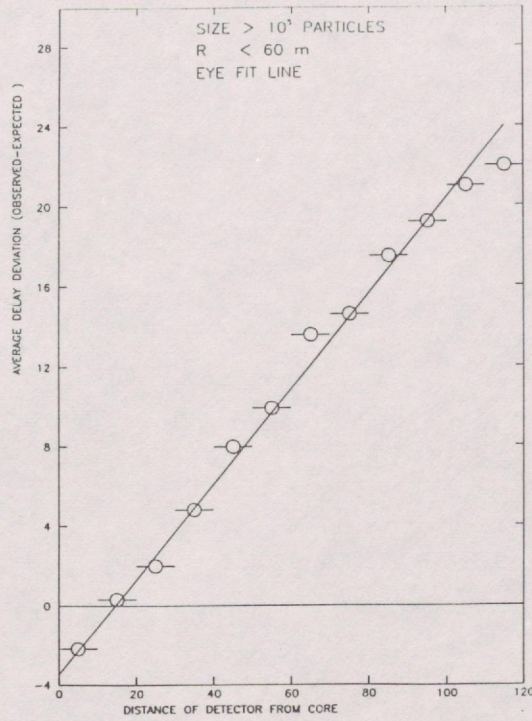


Figure 3. The dependence of the average deviation of the observed time delay in any detector from that of a plane passing through the core perpendicular to the shower axis, on the distance of the detector from the core.

small contribution from systematic errors in determining t_0 . In comparing the dispersions observed with calculations based on simulations care should be taken to subtract this effect from the data.

2.2. ESTIMATION OF SHOWER PARAMETERS

The conventionally used parameters of core position, size and age (NKG) of a shower are obtained by fitting the NKG function to the observed densities. The plane fit initial estimate of angle is used to transform the detector system to the shower plane and the NKG fit is done in the shower plane. Again one estimates the parameters by a minimization of the quantity χ^2 defined by

$$\chi^2 = \sum \omega_i (\Delta_i - D_i)^2 \quad (4)$$

where,

$$\Delta_i = N / (2 \pi r_0^2) g(s) (r_i / r_0)^{(s-2)} (1 + r_i / r_0)^{(s-4.5)} \quad (5)$$

the NKG function, r_i being the distance of the i th detector from the core (defined by the coordinates x_0, y_0), D_i being the density of particles observed in it. $g(s)$ is a ratio of gamma functions and is given by

$$g(s) = \Gamma(4.5-s) / [\Gamma(s) \Gamma(4.5-2s)]. \quad (6)$$

ω_i is determined by the measurement errors compounded with a Poisson spread in the number of particles expected in the detector. Since the ω_i s also are functions of the shower parameters to be estimated, the equations $d\chi^2/dx_0 = 0$, $d\chi^2/dy_0 = 0$, $d\chi^2/ds = 0$ and $d\chi^2/dN = 0$ form a system of

coupled non-linear equations and can be solved only iteratively. If one determined the parameters having all the four variables independently incremented, owing to the nature of the χ^2 surface, one often has N and s rather poorly determined, there being a large range of N and s over which $d\chi^2/dN$ or $d\chi^2/ds$ are small. To avoid this we have used the fact that the N and s derivatives will form a linear pair of equations, within a certain approximation to be described later, and can be solved to give the best fit N and s for a given core location. So in our parameter estimation the core location is obtained by an iterative minimization of χ^2 as in (4), and at each point determining the best fit N and s by a linear least-square fit. The NKG function can be rewritten as

$$\ln(\Delta_1) = K + s \{ \ln(r_i/r_0) + \ln(1 + r_i/r_0) \} + 2 \ln(r_i/r_0) + 4.5 \ln(1 + r_i/r_0) \quad (7)$$

Given the core coordinates, the array is divided into annular bins around the core and the average density of particles and the average distance are determined. This set of average densities is used to fit the function given by equation (5). In order that the problem remain linear, one has to ignore terms having the derivative $dg(s)/ds$, noting that

$$K = \ln(N / 2 \pi r_0^2) + \ln(g(s)) , \quad (8)$$

and also that the weights for each region be determined by the average observed densities. Thus the four shower parameters are determined by this hybrid iterative-LSQ procedure. The procedure has been tested with the help of artificially generated set of NKG showers.

A brief summary of the analysis procedure is as follows.

- 1) Obtain set of densities and times of arrival from the detectors in the array (these are either experimental data or artificial NKG data).
- 2) Use the seven highest density detectors (19 in case the highest is outside the 60 m ring) and fit a plane front to determine zenith and azimuth angles.
- 3) Use the angles estimated in (2) to estimate the shower core, size and age, by the hybrid procedure.
- 4) Using the shower core position determined in (3), refit the timing information from all the detectors to a conical front and re-estimate the zenith and azimuth angles.

2.3. ERRORS ON ESTIMATED PARAMETERS AND DIRECTION

Using a set of 'artificial' NKG showers, we find that the accuracy of core location is on the average 3.5 m, that of the age parameter 0.12 and the fractional error in size 20%. These refer to showers with size exceeding $5 \cdot 10^4$ particles and averaged over a uniform age distribution and with randomly located cores in the array. Fig. 4 shows the error in the space angle and one can see that 90% of the showers lie within a cone of half angle 2.2° from the true direction.

2.4. EFFICIENCY OF SHOWER DETECTION

In all the analysis we have imposed selection criteria on the showers before they are accepted for analysis. In addition to the hardware trigger we demand at least one detector among the innermost 61 to have recorded at least 4 particles in it and that a 'hexagon' of detectors have valid timing information in them. The efficiency of detection of showers was determined using 'artificial' NKG showers. The efficiency for detection depends on the core position, size and age of the shower and we find that showers of size exceeding $8 \cdot 10^4$, arriving up to a zenith angle of 60° and

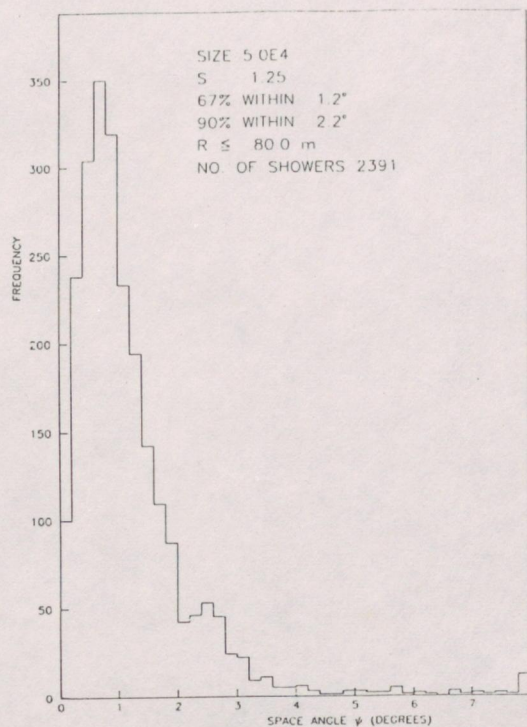


Figure 4. Distribution of the space angle between the estimated arrival direction and the true one. Results are based on artificial NKG showers.

having NKG age less than 1.6 are detected with an efficiency exceeding 90% up to 80 m from the center of the array.

2.5. DETERMINATION OF BACKGROUND FOR POINT SOURCES

Air showers have a fairly sharply falling zenith angle distribution and therefore when one is interested in tracking a particular source and study its time dependence compared to background events care should be taken to make sure that the source and the background have the same zenith angle coverage (Bhat *et al*, 1985). We have done this in the following way. At any instant we know the position of the source in the sky *viz* its zenith angle θ_s and azimuth ϕ_s . For an angular acceptance θ_a , we can draw an annulus in the sky formed by the rings with $\theta = \theta_s - \theta_a$ and $\theta = \theta_s + \theta_a$. At any instant we accept only events from this annulus and call them 'source' events if the space angle they make with the source is less than θ_a and 'background' otherwise. Since the background events come from a larger solid angle they are weighted in the ratio of 'source' solid angle to the 'background' solid angle. This ensures that the zenith angle and phase coverage is the same for both source and background, and gaps in run time or short run times do not matter.

2.6. DETERMINATION OF NUMBER OF MUONS IN A SHOWER

The passage of a single muon through the detector will have proportional counters in both the layers of the detector showing a minimum ionizing particle. The angle of the track is not so well determined because each counter is 10 cm wide and the two layers are separated by only 50 cm. However, we have looked at isolated single tracks from the data, and found that the track angle is always consistent with that of the shower. For parallel tracks we have developed an algorithm to

remove isolated hits and count the number of matched tracks whose angles are consistent with that of the shower and call that the number of muons in that detector. The location of the detectors is such that the average number of detectors which show at least one muon in them is 2.6 for showers landing within 80 m of the center, with size exceeding $8 \cdot 10^4$. The proportional counters are instrumented for pulse height measurement and hadronic cascades can also be identified.

3. Preliminary Results

3.1. RESULTS ON CYGNUS X-3

Data collected between October 1984 and January 1987, amounting to an effective running time of $4 \cdot 10^6$ seconds have been analysed using a slightly different procedure from that outlined in section 2.1. In step 1 we use all the timing information with weights given only by the detector resolution and fit a plane front. Step 4 uses a similar plane front fit using the Linsley function for the spread in arrival times as a function of core distance to determine the weights. Thus for showers that land at the edge of the array there could be a systematic shift in the estimated arrival angle. However, we find that a cone of half angle 1.5° still would contain 50% of the showers from a source. In this period we have observed 387 events from a cone of half angle 1.5° around Cygnus X-3, while the estimated background is 396.6; clearly no excess of events is seen. Fig. 5 shows the phasogram for all the events using the van der Klis and Bonnet- Bidaud (1981) ephemeris. There is no significant departure from uniformity. Based on this null result we set a 3σ upper limit for the steady flux from Cygnus X-3 as

$$f(E_0 > 5 \cdot 10^{14} \text{ eV}) < 9.5 \cdot 10^{-14} \text{ cm}^{-2} \text{ s}^{-1}$$

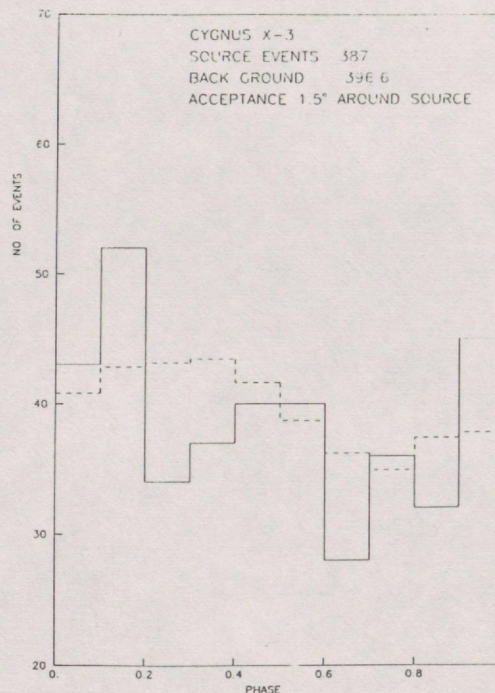


Figure 5. Phasogram of events within 1.5° of Cygnus X-3.

— Source
 - - - Background

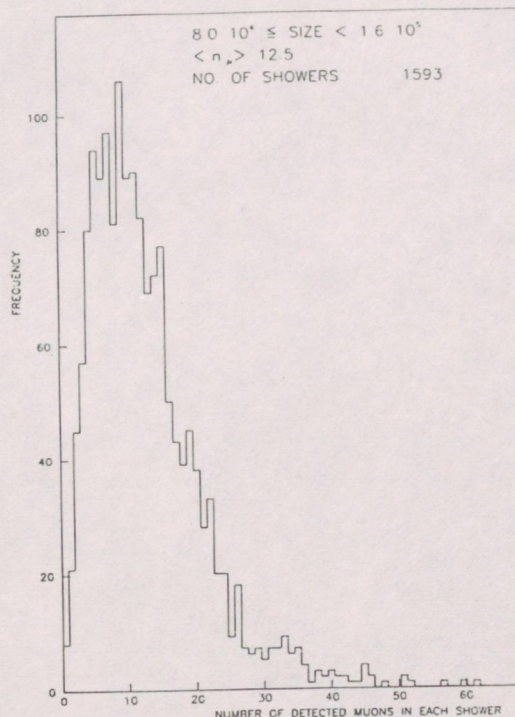


Figure 6. Distribution of total number of muons recorded in showers of size $8 \cdot 10^4 - 1.6 \cdot 10^5$ particles

Analysis of the data imposing different cuts, in size, age etc, is in progress. Time dependent signals (bursts) are being looked for and will form the subject of later work. Fig. 6 shows the distribution of the number of muons detected in each shower for data collected after April 1986. As can be seen for the background showers (non-gamma ray originated) we detect enough muons in each shower so that we can make cuts on the number of muons detected and improve the signal to noise ratio. For showers of size between $8 \cdot 10^4$ and $1.6 \cdot 10^5$ particles, we see that the average number of detected muons is 12.5. If we select showers with 0 or 1 muons, the background will be reduced by a factor of 55.

4. Conclusions

We have presented preliminary results from the KGF array on Cygnus X-3, not finding any excess in that direction. The phasogram also appears to be uniform. Analysis for time dependent signals, and using the muon detectors to increase signal to noise ratio is in progress.

Acknowledgements

We thank B.K.Chatterjee, A.V.John, R.Mahalingam, B.K.Nagesh, N.S.Prasad, Ramesh Babu Raj, Shobha Rao, V.Ramu, C.V.Raisinghani, A. Reddy, P.Reddy, A.J.Stanislaus, S.Swaminathan, Suresh Upadhyaya, P.Unnikrishnan, M.Venkateshwarlu, B.L.Venkatesh Murthy and R.P.Verma for their assistance in building and operation of the array and analysis of data. It is a pleasure to acknowledge the kind cooperation of Shri P.D.Gupta, Chairman and Managing Director of Bharat Gold Mines and his staff.

References

- Bhat P.N., Rajeev M.R., Ramana Murthy P.V., Rao M.V.S., Sinha S., Sreekantan B.V., Tonwar S.C. and Vishwanath P.R., *Techniques in Ultra High Energy Gamma Ray Astronomy*, Editors Protheroe R.J. and Stephens S.A. (University of Adelaide), 1, 1985.
- Bhat P.N., Khairatkar S.G., Rajeev M.R., Rao M.V.S., Sinha S., Sivaprasad K., Sreekantan B.V., Tonwar S.C., Vishwanath P.R. and Viswanathan K., *Very High Energy Gamma Ray Astronomy*, Editor Turver K.E. (D. Reidel Publishing Company), 271, 1986.
- Eames P.J.V., Lambert A., Perret J.C., Reid R.J.O., Smith N.J.T., Watson A.A. and West A., *Proc. XX ICRC*, Moscow, 2, 449, 1987.
- Linsley J., *Proc. XIX ICRC*, La Jolla, 3, 461, 1985.
- van der Klis, M. and Bonnet-Bidaud, J.M., *Astron. Astrophys.*, **95**, L5, 1981.

UHE GAMMA RAY OBSERVATIONS WITH THE KGF AIR SHOWER ARRAY

B.S.ACHARYA, P.N.BHAT, S.G.KHAIRATKAR, M.R.RAJEEV, M.V.S.RAO, S.SINHA*, K.SIVAPRASAD, B.V.SREEKANTAN, S.C.TONWAR, P.R.VISHWANATH AND K.VISWANATHAN

Tata Institute of Fundamental Research, Homi Bhabha Road, Colaba, Bombay 400 005, India

Results on search for point sources based on the data collected from October 1984 to January 1987 from the EAS array at KGF are presented. The array has a pointing accuracy of better than 1.5° to look at point sources. We present upper limit on the long term flux of gamma rays from Cygnus-X3 and report possible episodic emission from Cyg X-3 and Her X-1 during 1985.

1. INTRODUCTION

Since the discovery of Cyg X-3 as a ultra high energy (UHE) gamma ray source by the Kiel group¹ and subsequent confirmation by the Haverah Park group², search for such sources has gained importance as these are the likely sources of cosmic rays also. We have been operating an extensive air shower array specially designed to look for such sources since the end of 1984. We present here the salient features of the array and the results obtained so far.

2. EXPERIMENTAL SET UP

For a proper study of point sources of UHE gamma rays an EAS array should have the following features:

- (i) determination of the arrival angle of showers with a high accuracy,
- (ii) large collection area and
- (iii) large area muon detectors to establish the nature of the radiation.

An array with all these features has been operating at Kolar Gold Fields, India. The array^{3,4} consists of 127 plastic scintillation detectors, each of 1 m^2 area and 7 muon detectors of threshold energy 1 GeV, each having an area of 28.8 m^2 . The scintillators are arranged in a hexagonal pattern with a spacing of 20 m between

neighbouring detectors. The detectors extend up to 120 m from the center, covering an area of $4.3 \cdot 10^4 \text{ m}^2$. The innermost 61 detectors are instrumented for both timing and density measurements while the rest measure only density. The threshold particle density for triggering the timing detector is kept at 0.3 to minimize rise time effects. The air shower trigger is provided by a coincidence of any three (among the innermost 61) neighbouring detectors forming an equilateral triangle of side 20 m, in which the particle density exceeded 1.5. The trigger rate is 1 Hz. A stable 5 MHz Oscillo-quartz crystal provided real time information with an uncertainty of about 1 ms. Six of the muon detectors are located at the vertices of a hexagon of side 60 m and the seventh at its center, which coincides with the center of the array. Each muon detector consists of two layers of 48 proportional counters each, located under 600 g cm^{-2} of concrete and separated by 4 radiation lengths of brick. An on-line LSI-11 microprocessor recorded the events and also continuously monitored the performance of all the detectors.

The data used in the present work was collected from October 1984 to January 1987, during which only the innermost 61 detectors were operating with an enclosed area of $1.6 \cdot 10^4 \text{ m}^2$ and the muon detectors were not yet fully commissioned.

* Present address: Technical Physics Division, ISRO Satellite Center, Airport Road, Vimanapura P.O., Bangalore 560 017.

3. METHOD OF ANALYSIS

Shower size, N_e , and age parameter, s , were determined for each event in the usual way by fitting the Nishimura-Kamata-Greisen (NKG) function for the lateral distribution of electrons to the observed densities of particles. The arrival direction was obtained by fitting a plane shower front to the observed time delays taking into account the variation of disc thickness with core distance. The angular accuracy of the array was obtained by comparing the estimated zenith angles of the same set of showers using two separate groups of timing detectors (the odd numbered and the even numbered detectors) which spatially overlap. The angular accuracy thus obtained is 0.5° in zenith angle for showers of size $> 5 \cdot 10^4$ particles. Details of the analysis were given elsewhere^{3,4}. However, analysis of showers generated artificially with observed curvature but analysed with a plane front, has shown that 50% of showers are contained in a cone of half angle 1.5° around the true direction and 90% within 3° .

3.1. Estimation of background

Air showers have a fairly steep zenith angle distribution and therefore when one is looking for excess events from the source compared to background, care should be taken to make sure that the source and the background events are collected during the same time (to take care of run gaps) in the same zenith angle interval³. We have done this in the following way. At any instant we know the position of the source in the sky viz its zenith angle θ_s and azimuth ϕ_s . For an angular acceptance θ_a , we can draw an annulus in the sky formed by the rings with $\theta = \theta_s - \theta_a$ and $\theta = \theta_s + \theta_a$. At any instant we accept only events from this annulus and call them 'source' events if the space angle they make with the source is less than θ_a and 'background' otherwise. Since the background events come from a larger solid angle they are weighted in the ratio of 'source' solid angle to the 'background' solid angle. This ensures that the zenith angle and phase coverage is the same for both source and background, and gaps in run time or short run times do not matter. As the solid angle for the background events is about 40 times

larger than that for the source events, the background was determined with high statistical accuracy.

For further analysis, showers whose cores were within 70 m from the centre of the array and zenith angles less than 50° were accepted. Since the sources cover a wide zenith angle region, showers of a given observed threshold size but arriving at different zenith angles correspond to different primary energies since they develop through different atmospheric depths. While this does not affect the background estimates since it is calculated using showers recorded in the same zenith angle region during the same time as the source events, the threshold primary energy becomes ill defined. In order to avoid this, a vertical equivalent size (VES) is calculated for each shower using an absorption mean free path of 185 g cm^{-2} . Showers with $\text{VES} > 1.5 \cdot 10^5$, for which the array is fully efficient, were accepted for further analysis. The corresponding primary energy is $1.6 \cdot 10^{15} \text{ eV}$.

4. RESULTS

4.1. Cygnus X-3

Data collected over the entire period under consideration do not show any excess from the direction of the source, with $\theta_s = 3^\circ$. The number of events from the direction of the source is 1598 against an expected background of 1704.4, leading to a 2.6σ deficiency. The 3σ upper limit, based on this observation during the period October 1984 to January 1987, for the time averaged flux of gamma rays of energy $> 1.6 \cdot 10^{15} \text{ eV}$ is $1.8 \cdot 10^{-14} \text{ cm}^{-2} \text{ s}^{-1}$. The phasogram obtained using the van der Kluis ephemeris is shown in Fig. 1. There is no significant excess in any of the phase bins.

However, during April - May 1985, the number of events from the source direction is 207 while the background is 191.7, amounting to a 1.1σ excess. The phasogram for this period is shown in Fig. 2. In the phase bin 0.5 - 0.6, the number of source events is 38 and the background is 21.2, leading to a 3.7σ excess. All the 16 events in the DC excess appear in the phase excess. Considering that there are 17 such two month periods in the data and 10 phase bins, the overall

chance probability is 0.02.

4.2. Her X-1

Data collected over the entire period under consideration do not show any significant steady excess (121

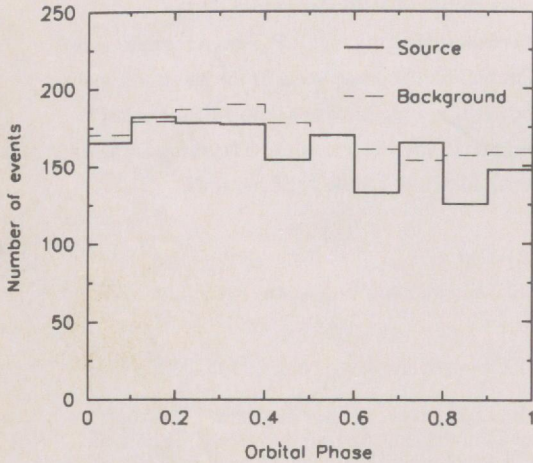


Fig. 1. Orbital Phsogram of air showers arriving from the direction of Cygnus X-3 during the period October 1984 to January 1987. No significant excess is seen in any of the phase bins.

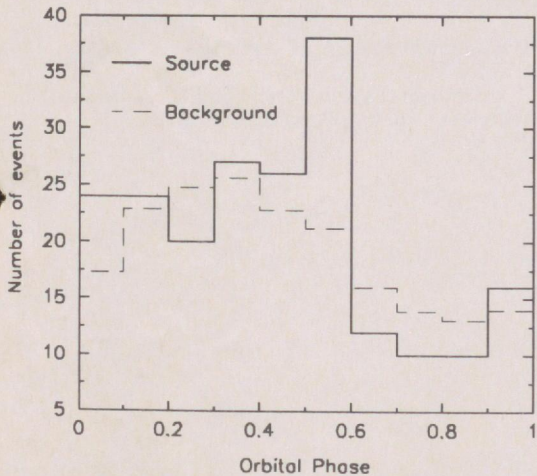


Fig. 2. Orbital phsogram of air showers arriving from the direction of Cygnus X-3 during the period April - May, 1985. A 3.7σ excess is seen in the phase bin 0.5 - 0.6. The overall chance probability, taking all degrees of freedom into account, is 0.02.

source events against an expected background of 113.8) or excess in any orbital phase region. To look for short episodes of activity, the data were divided into 6 roughly equal groups, essentially decided by the number of tapes on which they were written. In one of these groups comprising of 17 runs covering the period May 23, 1985 to July 20, 1985, the number of events within 1.5° from the source direction is 20 against a background of 10.5 events amounting to a 3σ excess over the background. The orbital phsogram for these events obtained using the ephemeris given by Voges et al⁵ ($p = 1.70016799$ d with phase, $\Phi = 0$ at epoch JD 2 443 357.8711) is shown in Fig 3. There are 7 events in the phase bin 0.7-0.8 against an expected background of 1.3 events. The Poisson probability that this occurrence is due to chance is $4.4 \cdot 10^{-4}$. Considering that there are 10 phase bins and 6 data sets, the probability of one or more phase bins showing such an excess in the entire data is $60 \times 4.4 \cdot 10^{-4} = 0.026$. It may be noted that out of the nine events in the steady excess, six are in this phase bin.

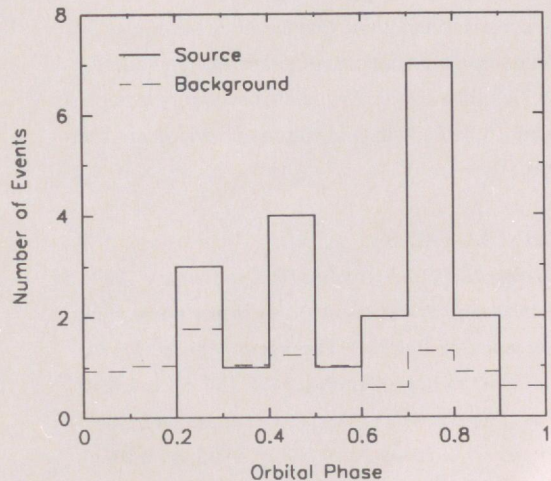


Fig. 3. Orbital phsogram of air showers arriving from the direction of Hercules X-1 during the period May 23 to July 20, 1985. There are 7 events in the phase bin 0.7 - 0.8 against an expected background of 1.3. The overall chance probability, taking all degrees of freedom into account, is 0.026.

It is interesting to note that the orbital phase interval 0.7-0.8 occurred only on two days, on May 24 and June 22, 1985 at 35-day phases of 0.095 and 0.923, just around the onset of 'High On' state, and on both these days excess events from the source are seen. The respective source and background events on these two days are 4, 0.23 and 3, 1.09. Thus it appears that Hercules X-1 is active in emitting UHE gamma rays in this orbital phase during May 23, 1985 to July 20, 1985.

With 6 events recorded in the phase interval 0.7-0.8 during an on-source time of 55.34 hours over an area of $1.54 \cdot 10^8 \text{ cm}^2$ and with 50% of the source events contained within the accepted angular region of 1.5° around the source direction, the time averaged flux of gamma rays of energy $> 1.6 \cdot 10^{15} \text{ eV}$ is estimated to be $(3.9 \pm 1.6) \cdot 10^{-13} \text{ photons cm}^{-2} \text{ s}^{-1}$. The corresponding source luminosity is $2.9 \cdot 10^{36} \text{ ergs s}^{-1}$, assuming isotropic emission and a source energy spectrum of $E^{-2} dE$ with a high energy cut off of 10^{16} eV . The exposure time for the phase interval 0.7-0.8 was 4.12 hours and the flux and luminosity during this phase interval are $5.2 \cdot 10^{-12} \text{ cm}^{-2} \text{ s}^{-1}$ and $3.9 \cdot 10^{37} \text{ ergs s}^{-1}$ respectively.

It is interesting to note that the most significant episode of pulsed emission of gamma rays of energy $> 0.6 \text{ TeV}$ seen by the Whipple Observatory group^{6,7} is on June 16, 1985, which is within our period of observation.

5. CONCLUSIONS

During the period October 1984 to January 1987, we have not seen any excess in DC or in any phase from the direction of Cyg X-3. The 3σ upper limit for the flux of gamma rays of energy $> 1.6 \cdot 10^{15} \text{ eV}$ is $1.8 \cdot 10^{-14} \text{ cm}^{-2} \text{ s}^{-1}$. There seems to be episodic emission in the phase 0.5 - 0.6 during April - May, 1985, with a significance of 0.02. There appears to be episodic emission from Her X-1 also during May 23 to July 20, 1985 in the orbital phase 0.7 - 0.8 just at the onset of the 'High On' state.

ACKNOWLEDGMENTS

We thank B.K.Chatterjee, A.V.John, R.Mahalingam, B.K.Nagesh, N.S.Prasad, Ramesh Babu Raj, Shobha Rao, V.Ramu, C.V.Raisinghani, A. Reddy, P.Reddy, A.J.Stanislaus, S.Swaminathan, Suresh Upadhyaya, P.Unnikrishnan, M.Venkateshwarlu, B.L.Venkateshamurthy and R.P.Verma for their assistance in building and operation of the array and analysis of data. It is a pleasure to acknowledge the kind cooperation of the Chairman and Managing Director of Bharat Gold Mines Limited and his staff.

REFERENCES

1. M.Samorski and W.Stamm, *Ap. J. Lett.*, 268 (1983) L17.
2. J.Lloyd-Evans et al., *Nature*, 305 (1983) 784.
3. P.N.Bhat et al., in *Techniques in Ultra High Energy Gamma Ray Astronomy*, eds. R.J.Protheroe and S.A.Stephens (University of Adelaide, 1985) pp. 1-7.
4. P.N.Bhat et al., in *Very High Energy Gamma Ray Astronomy*, ed. K.E.Turver (Reidel, 1987) pp. 271-274.
5. W.Voges, P.Kahabka, H.Ögelman, W.Pietsch and J.Trümper, *Space Science Rev.*, 40 (1985) 339.
6. P.W.Gorham et al., *Ap. J. Lett.* 308 (1986) L11.
7. P.W.Gorham et al., in *Very High Energy Gamma Ray Astronomy*, ed. K.E.Turver (Reidel, 1987) pp. 125-130.